

RSC Advances



This is an *Accepted Manuscript*, which has been through the Royal Society of Chemistry peer review process and has been accepted for publication.

Accepted Manuscripts are published online shortly after acceptance, before technical editing, formatting and proof reading. Using this free service, authors can make their results available to the community, in citable form, before we publish the edited article. This *Accepted Manuscript* will be replaced by the edited, formatted and paginated article as soon as this is available.

You can find more information about *Accepted Manuscripts* in the [Information for Authors](#).

Please note that technical editing may introduce minor changes to the text and/or graphics, which may alter content. The journal's standard [Terms & Conditions](#) and the [Ethical guidelines](#) still apply. In no event shall the Royal Society of Chemistry be held responsible for any errors or omissions in this *Accepted Manuscript* or any consequences arising from the use of any information it contains.

Mechanistic Approach on Heat Induced Growth of Anionic Surfactant: A Clouding Phenomenon

Arti Bhadoria^a, Sugam Kumar^b, Vinod K. Aswal^b and Sanjeev Kumar^{a*}

^aSoft Material Research Laboratory, Department of Chemistry, The Maharaja Sayajirao University of Baroda, Vadodara 390 002, India.

^bSolid State Physics Division, Bhabha Atomic Research Centre, Trombay, Mumbai 400 085, India

ABSTRACT

Different anionic surfactants: tetra-*n*-butylammonium dodecylsulphate (TBADS), tetra-*n*-butylammonium- α -sulfonato myristic acid methyl ester (TBAMES) and tetra-*n*-butylphosphonium dodecylsulphate (TBPDS) are synthesized. Though all the surfactants are ionic in nature, they show clouding phenomenon on heating. Effect of temperature on the solution behaviour (micellization and clouding) of synthesized surfactants has been studied by conductometry, dynamic light scattering (DLS), nuclear magnetic resonance (NMR) techniques, small angle neutron scattering (SANS) and polarising optical microscopy (POM) studies. Experimental cmc data of TBADS show U shaped curve when plotted against temperature. Conductivity measurements follow different trends with temperature for various fixed concentrations of TBADS. Conductivity increases with temperature at lower TBADS concentration while an unusual decrease was observed (with temperature) for higher TBADS concentration. NMR data with temperature also show similar peculiarity as observed conductometrically. The broadening and splitting of NMR peaks with increasing temperature is in agreement with the growth of micelles and formation of two morphologies. The grown aggregates tend to exhibit a stronger attractive potential relative to individual spherical micelles. Increase in δ (ppm) values along with the broad peaks in NMR on increasing temperature corroborates the dehydration of counterion and the increase in attractive forces among the grown aggregates. This proposition has been supported by DLS and SANS results. It is experimentally confirmed that the formation of bigger aggregates through the fusion of grown micelles facilitated by the dehydrated counterion on increasing temperature and the onset of attractive interactions are the key processes involved in clouding phenomenon of ionic surfactant solutions. The Langer-Schwartz's nucleation theory and the growth of micelles beyond the critical droplet size resulting phase separation are confirmed through the POM results. Thus, the response of solution complements both with conventional ionic and nonionic surfactants depending upon the concentration/temperature. This added feature can be due to the substitution of Na^+ by a quaternary counterion in a typical anionic surfactant.

KEYWORDS: Ionic surfactant, temperature effect, growth, morphology, cloud point, phase separation, NMR, SANS, POM.

INTRODUCTION

The interfacial water in the immediate vicinity of hydrophobic and hydrophilic surfaces of amphiphile plays a predominant role in various phenomena.^{1,2} Hence, the knowledge of the factors affecting aggregate formation becomes important in the physical synthesis of self assemblies. It has been well understood that water molecules confined in various micro-heterogeneous nano confinements (like micelles, reverse micelles, liposome, lamellae etc.) behave in a markedly different manner compared to bulk water. The property of the confined water is dependent upon the nature of the surfactant molecule (ionic or nonionic) constituting a self assembly. The nonionic surfactants are believed to possess aqueous solubility due to hydrogen bonding between water and surfactant molecules which breaks on increasing the temperature resulting in a cloudy or turbid solution. This particular temperature is called cloud point (CP).^{3,4} CP being a principal feature of nonionic surfactant solution, it is uncommon with ionic surfactants due to the presence of electrostatic repulsions between the charged aggregates. Some ionic surfactants with high salt concentration, surfactant with large head group or large counter ions and some mixed cationic and anionic surfactant solution are known to show clouding phenomenon.⁵⁻¹⁰ Most of the studies with conventional anionic surfactants are carried out with TBA^+ counterion added externally or derived from the surfactant (tetra-*n*-butylammonium dodecylsulphate, TBADS) itself^{8,11-14} Recently, effects of addition of quaternary ammonium bromides on aggregation behaviour/structural transition of a few anionic surfactants have also been studied using various techniques.^{15,16} However, detailed morphological transition resulting due to heating remains nearly unexplored on the molecular level. A fair discussion regarding morphological aspects for the clouding phenomenon of nonionic surfactants can be found in a recent review.¹⁰ However, very little is known regarding the morphologies present in ionic surfactant solutions below and at/above the CP. Different kinds of assemblies can be transformed in response to variations in environmental factors. Temperature plays an important role in such transitions.^{17,18} Usually the transition from a higher order aggregate to a lower order state on increasing the temperature takes place.¹⁹⁻²¹ Among the ionic surfactants, micellar growth behaviour on heating is common only for some cationic surfactants mixed with oppositely charged

surfactant/hydrotropes.^{17, 22,23} However, studies of the temperature induced micellar growth are so far rare for single anionic surfactant system. Therefore some key questions need to be addressed in order to understand the rationale behind the morphology and solution behaviour. Different models like the onset of attractive interactions, multiple bridging among the ionic micelles through alkyl tails of counterion, formation of the connected micellar network or strongly orientation dependent interactions between water and micellar head groups, without any experimental evidence, have been employed to provide the mechanism resulting into the clouding phenomenon.^{14, 24-28} Still most of the time discussion regarding the mechanism of clouding phenomenon in charged micellar solutions ended with a hazy picture.^{5, 8, 24,29-34} Here, attempt has been made to rationalize the observations and provide experimental evidences along with qualitative arguments regarding the solution behaviour of typical anionic surfactants and the morphological transitions involved therein below and above CP using various physicochemical techniques. For the purpose different anionic surfactants having quaternary counterions: tetra-*n*-butylammonium dodecylsulphate (TBADS) tetra-*n*-butylammonium- α -sulfonato myristic acid methyl ester (TBAMES), tetra-*n*-butylphosphonium dodecylsulfate (TBPDS) have been synthesized.

Both micelles and grown aggregates coexist at (CP) and beyond CP. The potential application for grown aggregates can be for storage or controlled release applications (e.g in cosmetics, drug delivery etc). It has also been reported that loading of DNA into vesicles can greatly be improved by using micrometer-sized vesicles.³⁵ The clouding at low temperature and concentration may find use as cloud point extraction (CPE) systems in the extraction of various charged and thermally labile moieties.

EXPERIMENTAL SECTION

Materials. Sodium dodecyl sulphate, SDS ($\geq 99\%$), tetra-*n*-butylammonium bromide, TBAB, (99%), tetra-*n*-butylphosphonium bromide, TBPB (99%) and Triton X-100 (ultra) were purchased from Sigma St Louis, USA. α -sulfonato myristic acid methyl ester (MES), a gifted sample (Lion corporation, Tokyo), was recrystallized using dry ethanol before use. The present anionic surfactants have been prepared by mixing equimolar solutions of SDS /MES with TBAB/TBPB. The respective clear mixture was stirred at room temperature for 62h. The formed compound was then extracted with dichloromethane, DCM as solvent and finally after vacuum drying, the isolated viscous mass is used for further analysis. The purity of all the surfactants (tetra-*n*-butylammonium dodecylsulphate (TBADS), tetra-*n*-butylammonium

α -sulfonato myristic acid methyl ester (TBAMES) and tetra-*n*-butylphosphonium dodecylsulphate (TBPDS), was confirmed by ^1H NMR, IR, mass spectrometry and by surface tensiometry. Water used to prepare the aqueous surfactant solutions was double distilled in an all-glass distillation apparatus. The specific conductivity of the water was in the range $(2-4) \cdot 10^{-6} \text{ S}\cdot\text{cm}^{-1}$. D_2O used in the sample preparation for NMR is 99.9 atom % D purchased from Sigma-Aldrich St Louis, USA.

Experiments.

Conductometric measurements were carried out by using a conductivity meter EUTECH cyberscan CON510 (cell constant 1 cm^{-1}) with an inbuilt temperature sensor. A pre-calibrated conductivity cell was used to obtain specific conductance at an appropriate concentration range. Temperature of the sample solution was precisely controlled by SCHOTT CT 1650 thermostat with an accuracy of $\pm 0.1^\circ\text{C}$. The cell with an appropriate amount of the solvent (water) in a vessel was thermostated for at least 30 minutes prior to the measurement. The conductivity runs were carried out by adding concentrated surfactant solution to the solvent water. The critical micelle concentration (cmc) and degree of counterion dissociation (α) values for the synthesized anionic surfactants were determined from the intersection point between the two straight lines (in the plot of the [surfactant] vs. specific conductance (κ)), and the ratio of the slopes of the postmicellar to that of the premicellar portions of the straight lines.

The CP values were obtained by placing sample tubes, containing surfactant solutions with a fixed concentration into a temperature-controlling water bath. The onset of turbidity temperature (visual observation) was noted. The system was allowed to cool and temperature at which the disappearance of turbidity took place was also noted. The average of these two temperatures was taken as the cloud point (CP). This procedure was repeated for the same sample and nearly two concurrent values (within $\pm 0.1^\circ\text{C}$) were considered as the final CP. Similar CP measurements were made by diluting the samples using double distilled water to collect CP data at various concentrations.

DLS measurements were performed using a Brukhaven 90 plus particle size analyser. The solid laser operated at 660 nm with a maximum power output of 15 mW with the scattering angle 90° was used. The sample was filtered ($0.22 \mu\text{m}$) to avoid interference from dust particles. The correlation functions were analyzed by the method of Contin and Cumulant to have an idea of mean diameter and polydispersity index.

NMR spectra were obtained with Bruker Avance 400 Spectrometer at different

temperatures (20-70°C). All the surfactant solutions were prepared in D₂O. About 0.6 ml of solution was transferred to a 5 mm NMR tube and chemical shifts were recorded on the δ (ppm) scale.

SANS measurements were carried out using a SANS spectrometer at Dhruva Reactor, Bhabha Atomic Research Centre, Trombay, India.³⁶ The samples were placed in a quartz sample holder of thickness 2mm with the varying temperature below and above CP. The measured SANS data have been corrected and normalized to an absolute scale using standard procedure.^{26, 37} In SANS measurements one measures coherent differential scattering cross-section per unit volume ($d\Sigma/d\Omega$) as a function of scattering vector $Q(=4\pi\sin\theta/\lambda)$, where 2θ is the scattering angle and for monodisperse micelle solution it can be expressed as³⁸

$$d\Sigma/d\Omega = n_m V_m^2 (\rho_m - \rho_s)^2 \{ \langle F^2(Q) \rangle + \langle F(Q) \rangle^2 [S(Q) - 1] \} + B. \text{-----} \quad (1)$$

Where n_m and V_m are the number density and volume, respectively, of micelle, $F(Q)$ is the single particle form factor that depends upon shape and size of particle, $S(Q)$ is the interparticle structure factor and B denotes incoherent scattering background contributed from hydrogen in the micelle. The dimensions (semimajor axis (a), semiminor axis ($b=c$)), aggregation number, $N(=4\pi ab^2/3v)$, where v is the volume of the surfactant tail) and the average charge of micelles have been determined from the analysis. The relevant expressions used are similar as reported earlier.^{26,27}

To get the visual observations, experiments were performed using a leica DFC 295 optical microscope fitted with Leica (Germany) Lens (4X, 10X, 20X and 50X magnification). Images are recorded using inbuilt leica camera at 20X. The temperature was maintained, using linkam heating stage LST 420 controlled by Leica application suite computer software LAS-V41.

RESULTS AND DISCUSSION

The micellar surface is characterised by the presence of water of hydration. The quaternary counterion TBA⁺/ TBP⁺ (from the surfactant itself), in addition to the positive charge, carries four butyl chains. Therefore, it can interact hydrophobically with the alky chains of the surfactant molecules, constituting the micelle, as well as electrostatically with oppositely charged micellar head groups. The butyl chains of such counter ions can get embedded between the monomers of the micelle due to hydrophobic interactions. Also, due to bulky nature of the counterion, the micellar surface can quickly be saturated with TBA⁺/ TBP⁺ and remaining ones may be used in linking various micelles together resulting bigger aggregates

giving clouding.⁸ The micellar parameters³⁹ and CP data for the synthesized surfactants are acquired by the procedure given under experimental section.

Effect of Temperature on Micellar Parameters

To understand the clouding behavior of quaternary counterion surfactants, cmc data have been compared for the surfactants having Na⁺ and quaternary counterions. The cmc values are higher for surfactants having inorganic counter ion (e.g. Na⁺) than the surfactants containing quaternary organic counter ion, TBA⁺ or TBP⁺ (Table T1, supporting information). The electrostatic as well as hydrophobic interactions may force organic counter ion to bind with the micellar surface and initiate the phenomenon of micellization at lower concentration. However, cmc value is found higher for TBPDS than TBADS. The electrostatic repulsive interaction between similar charged head groups will also be less depleted with TBP⁺ than TBA⁺ resulting in higher cmc values for TBPDS.

Further, TBADS is chosen for detailed micellization study at different temperatures. Figure 1 shows the plots of κ vs [TBADS] at various temperatures. These plots are used to determine cmc and alpha values at different temperatures, summarized in Table 1. Cmc variation with temperature shows a U shaped behavior (Figure 2a). A detailed discussion on the U shaped behavior of cmc with temperature can be found in earlier report.⁴⁰ However, the temperature of minimum cmc (T_m) was found higher than that reported for conventional ionic surfactants (e.g SDS).⁴¹ The α value shows a gradual decrease with temperature (Figure 2b). The reported α data on conventional ionic surfactant suggest that α show a weak dependence on temperature.⁴² In another study, an increase in α is also been reported with temperature.⁴³ Above two observations (higher T_m and decreasing α) indicate that TBADS responds differently on heating. A similar hint was intimated from the literature by Bales and Zana.⁸

Table 1 cmc and α values for TBADS at different temperatures.

Temperature (°C)	CMC 10 ⁻³ (M)	α
25	1.22	0.42
30	1.21	0.39
35	1.19	0.37
40	1.16	0.37
45	1.18	0.37
50	1.25	0.37
65	1.42	0.23

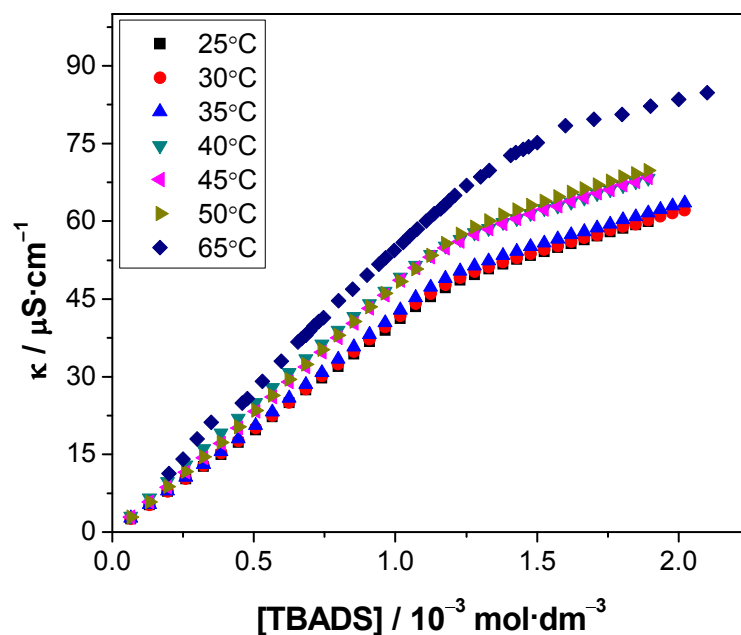


Fig. 1 Variation of specific conductance (κ) vs concentration plots for TBADS at different temperatures

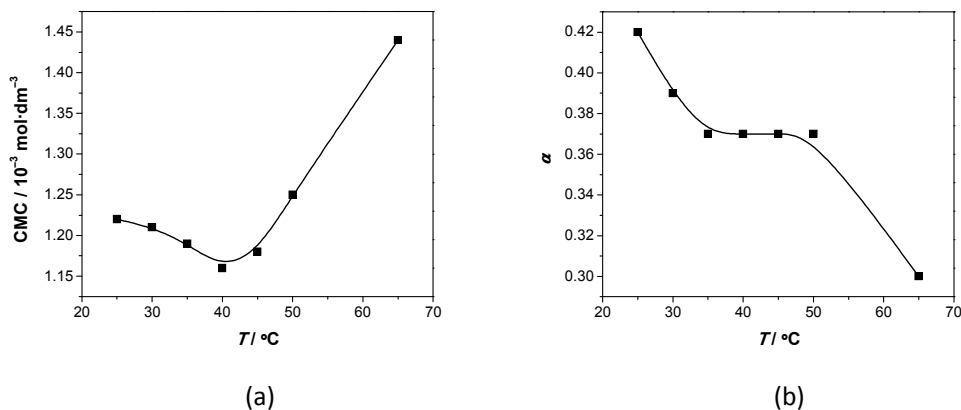


Fig. 2 Temperature effect on a) cmc and b) α of TBADS

To substantiate the heating response of quaternary surfactants conductivity data is collected at various temperatures for different TBADS concentrations as shown in Figure 3. Conductivity increases with the increase in temperature, for 0.005M TBADS concentration. This observation is in line to what we observed in Figure 1 as well as in earlier reports.⁴² When the conductivity experiments were performed with 0.015M TBADS, κ values showed a weak dependence (nearly constant) on temperature. However, conductivity data for 0.03M

TBADS showed a decrease in κ with temperature. This observation is in sharp contrast to the reported conductivity data for conventional ionic surfactants at higher concentration.⁴² It is hard to understand the decrease in conductance of a solution with temperature which contains charged species. Conductance in a typical solution generally depends upon mobility, number and ion sizes. The present decrease of κ with temperature (0.03M TBADS, Figure 2) can be understood in the light of the facts: a) both counterion (TBA^+) and headgroup will have certain degree of hydration which is expected to decrease on heating ; b) this dehydration of counterion and headgroup causes effective charge neutralization c) due to these reasons the charge of the conducting species (counterion and headgroup) may neutralize with a concomitant conversion into nearly non-ionic species. It can be mentioned here that quaternary counterions are less hydrated than inorganic counterions and the charge of the former can be considered to be buried in a paraffin shell. This may facilitate quaternary counterion to interact with anionic micelle electrostatically and hydrophobically. Interestingly, such pseudo-nonionic micelles were proposed to explain the clouding behavior of ionic surfactant system.⁵ The above discussion seems sufficient to understand the peculiar behaviour (higher T_m , decrease in α and κ) of quaternary surfactants with respect to temperature.

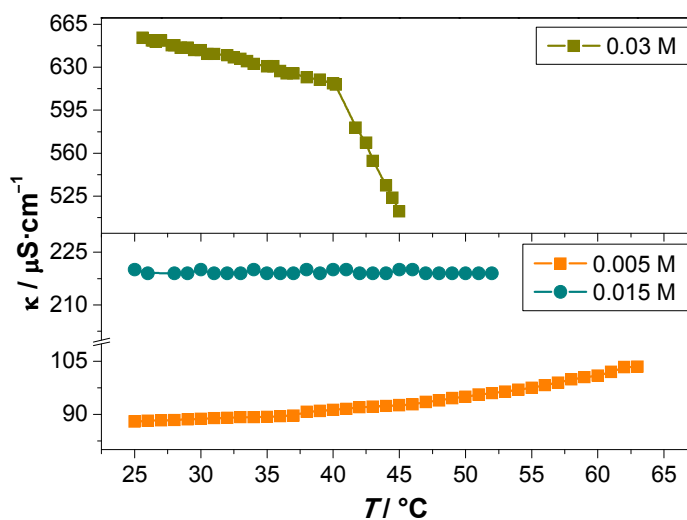


Fig. 3 Variation of specific conductance (κ) vs temperature plot for TBADS at different concentrations.

Clouding phenomenon in anionic surfactant solution.

A perusal of CP data as seen in Figure 4 indicates that CP follows the order: TBAMES>TBADS>TBPDS. This order results from various combinations of counterion and alkyl head group part of the surfactant. Among TBA⁺, TBAMES have higher CP than TBADS. TBAMES show clouding at higher temperature due to the presence of one ester group in addition to a sulfonate moiety in the head group. The extra ester group may form H-bond with water molecule due to dipole-dipole interaction resulting in increased hydration and is responsible for higher CP. The CP for TBPDS is found much lower than both TBADS and TBAMES surfactants. This may be due to the nature and bigger size of TBP⁺ counterion due to which the surface dehydration is expected more. At equal concentrations of TBADS and TBPDS, faster saturation of micellar surface is expected with TBP⁺ and thus more TBP⁺ are left to facilitate the approach of various micelles close to each other resulting in lower CP.

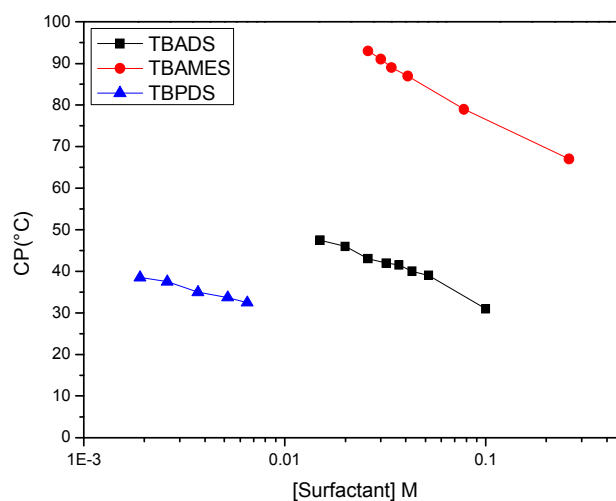


Fig. 4 Variation of cloud point (CP) at different surfactant concentrations.

To get an idea regarding the changes in micelle size with an increase in temperature, DLS studies were performed with various surfactant solutions at different temperatures (below and above the CP). It was observed that two populations of different sizes are present near the CP. This type of behaviour is already reported for other systems^{17,24,44} which indicates that presence of two types of micelles may be a general feature for ionic surfactants showing clouding. From the lognormal distribution it was intimated that effective hydrodynamic diameter of micelle increases considerably near CP (Figure 5a). Approach of grown micelle with other micelles may start, at a particular temperature which then leads to the formation of

bigger aggregates responsible for clouding phenomenon. At/after CP, two phases gradually separate and one of the two phases now spans the whole scattering volume. This is in consonance with the decrease in size after CP. The grown micelles have participated in linking, forming one phase of bigger aggregates responsible for clouding and the other phase contributing to scattering is now left with small sized micelles as seen from the Figure 5a. As the micelles are growing with increasing temperature, the ratio of the bigger micelles to that of smaller ones increases with the increasing temperature, leading to the increase in polydispersity initially. But after certain temperature, the micelles are grown and hence the ratio between two decrease, lowering the polydispersity, which is also an indication of one population dominating. Interestingly, the polydispersity of the system reaches to minimum, as the phase separation starts. It can be said that only one of the two phases now spans the whole scattering volume tending the system towards the mono-dispersed phase (Figure 5b).

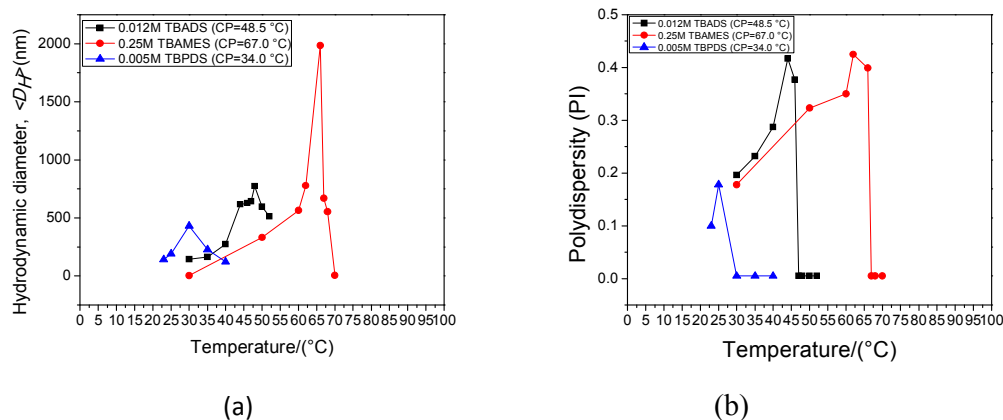


Fig. 5 Temperature effect on a) hydrodynamic diameter $\langle D_H \rangle$ and b) polydispersity (PI) of different surfactants solutions

Among various studies, the NMR spectroscopy is also found one of the suitable methods for the monitoring of interactions in micellar solution. Figures S1-S3 (supporting information) shows chemical structure and the ^1H NMR spectra of all anionic surfactants in D_2O . The ^1H NMR for all the above anionic surfactants at variable temperature (below, at and above CP) is acquired. The cropped ^1H NMR of representative 0.05M TBPDS (CP=27°C) at variable temperature shows the shifting of spectra to higher δ (ppm) scale as the temperature increases (Figure 6a). The decrease in the degree of hydration and electron density around N1, the counter ion (-P-CH₂) proton, near the micelle surface can easily be ascertained by the chemical shift analysis. The higher δ value corroborates the decrease in hydration and also

the onset of attractive interaction between the counterions and the micellar head group. The chemical shift of α -methylene protons, attached to the sulphate group is also significantly affected by the charge distribution around it (Figure S4, supporting information). Hence, due to the dehydration of counterion and the surfactant head group, the counterion condensation takes place which may be responsible for growth of the micelles. This may find support from the fact that Mitchell- Ninham parameter⁴⁵ ($P=v/a_h l$, where v and l are the volume and length of the alkyl part, respectively and a_h is the head group area of a typical surfactant) increases due to condensation of various counter ions with a simultaneous decrease in the value of a_h . The increase in P is always reported for the formation of higher order aggregates.²³ The overall micelle charge may also decrease leading towards the pseudo- nonionic system. To show the effect of counterion without the interference of other neighboring protons, ³¹P decoupled NMR at different temperatures was also acquired (Figure 6b). The N1 proton in TBPDS splits into two peaks at higher temperature. This is due to the alteration of the resultant chemical environment among the two types of micelle population. However, a gradual broadening of above peak on heating indicates the micelle growth^{24, 46} as the system approaches CP. Thus, the broadening and splitting of the peak hints about the micelle growth and ultimately the formation of bigger aggregates through the fusion of various micelles via dehydrated counter ions at higher temperature. Similar results are obtained for TBAMES (Figure S5, supporting information). This study was extended to TX-100, a well known conventional nonionic surfactant showing clouding on heating wherein no such broadening and splitting of peaks is seen on heating till CP. This may be due to the presence of more hydrophilic units present in the chain which on heating may only dehydrate and decrease the polar character of the poly(ethylene glycol) headgroup, giving rise to the attractive interactions responsible for clouding⁴⁷ (Figure S6, supporting information).

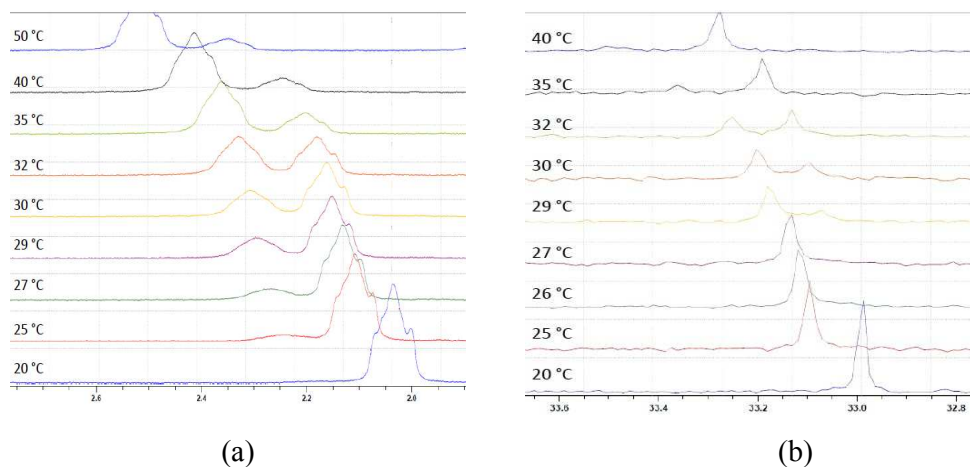


Fig. 6 NMR spectra a) ^1H and b) ^{31}P for 0.05M TBPDS at different temperatures below, at and after CP

To further examine the mechanism going on during the whole phenomenon, typical noninvasive 2D NMR studies were carried out for all anionic surfactants at room temperature (RT) and near CP. The results of two-dimensional nuclear overhauser effect spectroscopy (2D NOESY) enabled the identification of the counterion effects with the increase in temperature. Representative 0.03M TBADS (CP= 42.5°C) solution is selected here to show the heating effects. On heating clear cross peaks (absent in 2D COSY (Figure S7, supporting information and 2D NOESY at RT, Figure 7a) due to the dominating hydrophobic interactions occurring due to the dehydration at higher temperature along with the screening electrostatic ones between the TBA^+ counter ion and surfactant head group are seen (Figure 7b). Strong correlation cross peaks between N1-N4, N1-N3, N1-N2 and S1-N4, S1-N2 protons are seen on approaching CP, suggesting the intercalation of the counterion butyl chain with increasing temperature. Similar results are seen with 0.005M TBPDS (CP= 27.0°C) and 0.25M TBAMES (CP= 65.0°C) surfactant solutions (Figures S8-S9, supporting information) with the only difference in the signs of the cross peaks in TBAMES near CP. The signs of nuclear overhauser effects (NOE) of all the diagonal and the cross peaks in TBADS and TBPDS solutions at RT and near CP are positive, whereas the cross peaks for TBAMES solution near CP showed the opposite (negative NOE) to that at RT. This means for TBADS and TBPDS solutions near CP (lower than the CP for TBAMES) the TBA^+ / TBP^+ counterions are not completely dehydrated and hence the tumbling rate of the intercalated counterion chain in this case is fast giving positive NOE.¹⁵ For TBAMES solution near CP i.e at 64°C the motion of the alkyl part and the TBA^+ counterion is restricted at such high temperature due to the more insertion of TBA^+ (more dehydrated) into the hydrophobic core. Also the distinct cross peaks S2-S15, S2-N4 and more intense N1-N4, N1-N3 and N1-N2 (Figure S9, supporting information) are in agreement to the dominating hydrophobic effects. NOESY results corroborate the proposition that dehydrated TBA^+ / TBP^+ ions associate with alkyl heads via hydrophobic interactions to form grown micelles at higher temperature (near CP). TBA^+ / TBP^+ ions first attach to the surface of the anionic micelles and then on further dehydration at higher temperature become inserted into the hydrophobic core. Though, the NMR is not directly sensitive to the morphological transitions, these transitions can be assessed from NMR (from broadening and shifting of peaks) indirectly with the knowledge of other techniques.

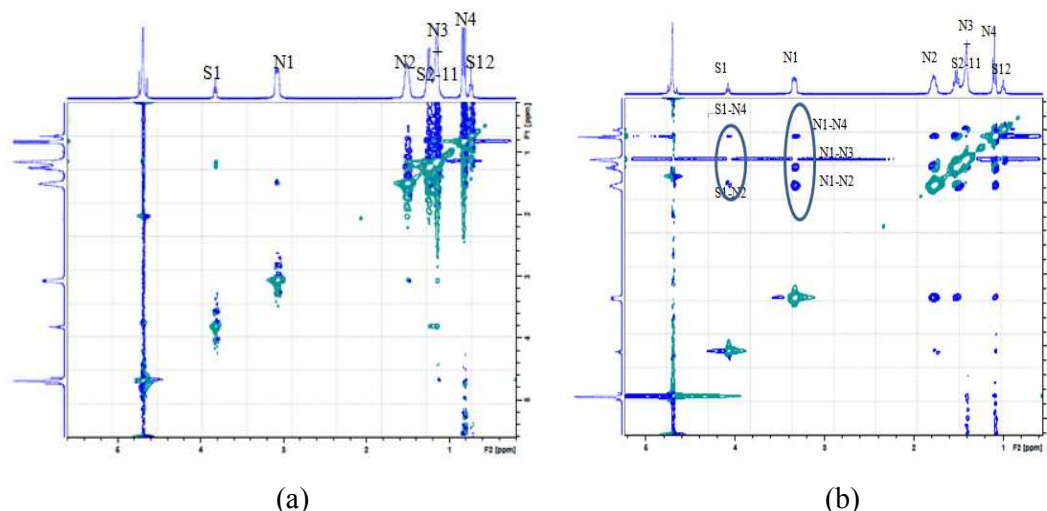


Fig. 7 2D NOESY NMR spectra of 0.03 TBADS at (a) 18°C and (b) near CP.

SANS measurements provide useful information pertaining to the micelle growth and fractional charge for different anionic surfactant solutions in a non-invasive manner. SANS spectra of 0.0124M TBADS as a function of temperature before and after the CP is shown in Figure 8. On increasing temperature the cross section decreases remarkably in low Q region. This is a typical behaviour observed earlier.^{24,27} The purpose of the present temperature effect study was to have enough temperature range below and above CP. Therefore, a lower concentration (0.0124M TBADS; CP=48.5°C) has been taken. No significant change was observed in fitted micellar parameters when the solution temperature reaches near CP (Table T2, supporting information). Once the CP crosses, magnitude of scattering intensity curve starts decreasing in the low Q region. This means the number density of individual micelles on heating decrease as the grown micelles fuses via butyl chains of dehydrated TBA⁺ and form bigger aggregates. These bigger aggregate sizes are expected to be out of range of the present SANS spectrometer. This actually is seen from the decrease in micellar fraction of individual micelles (which now spans the whole scattering volume) with the increase in temperature after CP. From earlier studies²⁶ it is seen that only 40% of the TBA⁺ counterions are adsorbed at the micelle surface due to their bulky nature. Also it was seen that only two butyl chains due to the geometric restrictions can intercalate into the micellar core and about 75% volume of these tail reside in the core. The intercalation of dehydrated TBA⁺/ TBP⁺ (at higher temperature near CP), between the anionic head groups screen the charge, reduce electrostatic repulsions between them, and hence the overall charge on micelle surface decreases (Table T2, supporting information) giving pseudo nonionic character.

The scattering from the individual micelles exist at and even beyond CP suggesting that only a part of micelles (grown) fuse via dehydrated counterions, forming bigger aggregates responsible for clouding (Figure 8). On further increasing temperature, more micelles grow and participate in forming bigger aggregates responsible for clouding resulting in further decrease of individual micelle fraction.

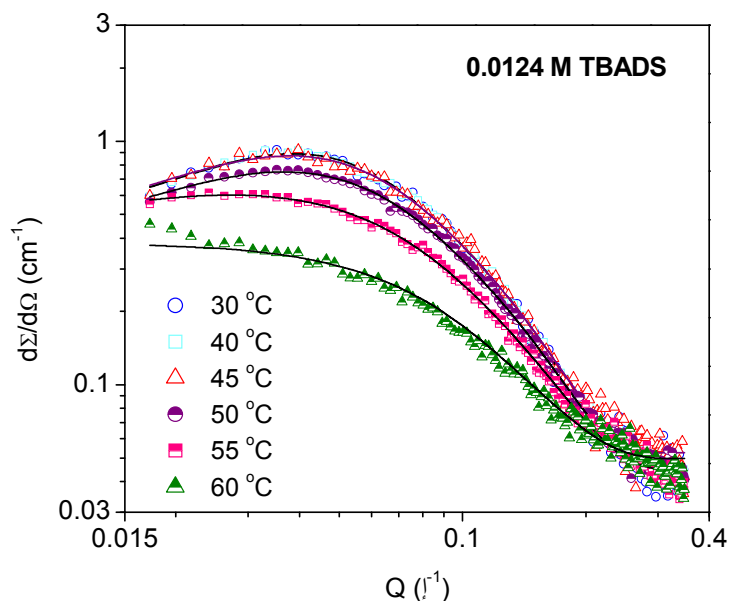


Fig. 8 SANS spectra of 0.0124 M TBADS at varying temperatures below and above CP.

To get further insight, the temperature effect is also studied with TBAMES. It gives clouding at higher temperature and at comparatively higher concentration than TBADS. SANS spectra of 0.25M TBAMES (CP=65°C) at various temperatures are shown in Figure 9. The TBAMES solution behaviour overlaps with both conventional ionic and non-ionic micellar solutions. The behaviour can be understood in the light of the fact that dehydrated TBA^+ counterion associate with ionic micelle to form grown micelles at higher temperature near CP and decrease the electrostatic interactions. This is clearly reflected by the lower α values. Table 2 contains fitted micellar parameters which show that length of semi-major axis (a) increases with temperature from 28.1 to 89.2 Å confirming the micelle growth on heating. The scattering intensity above the CP is now due the lower sized anionic micelles, which spans the whole scattering volume in the solution. Here, along with the micelle growth, the onset of attractive interaction is also confirmed from the low Q upturn (inset figure) with the increase in temperature. However, in earlier studies^{19, 48} micelle disintegration was reported for charged micelles on heating.

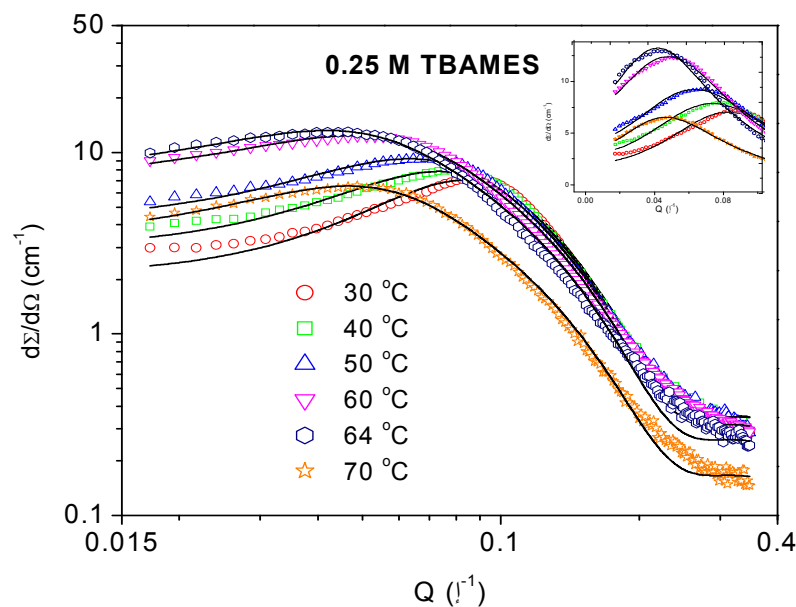


Fig. 9 SANS spectra of 0.25M TBAMES at different temperatures below and above CP

Table 2 Fitted micellar parameters of 0.25 M TBAMES at varying temperatures using model for prolate ellipsoidal.

Temperature (°C)	Semiminor axis $b=c$ (Å)	Semimajor axis a (Å)	Aggregation Number N	Fractional charge α	Micellar fraction (%)
30	16.0	28.1	50	0.06	100
40	16.0	30.5	54	0.06	100
50	16.0	35.6	62	0.05	100
60	16.0	50.7	87	0.04	100
64	16.0	89.2	151	0.03	100
70	16.0	81.8	139	0.01	48

SANS spectra for SDS, being a typical conventional anionic surfactant (not showing clouding) is shown in figure S10, (supporting information). From the fitted micellar parameters of 0.03M SDS solution (Table T3, supporting information) it is seen that ellipsoidal micelle disintegrate (decrease in semi major axis (23Å to 19.7Å) on increasing the temperature from 30°C to 60°C). While TX-100, a well known conventional non ionic surfactant showing clouding on heating, neither show any micelle growth nor the micellar shape change to be reflected in the above analysis. It is in consonance with the other results (theoretical as well as experimental) reported for TX-100.^{49,50} However, the low Q upturn

with increasing temperature due to the attractive interaction is the predominating factor responsible for clouding. (Figure S11 and Table T4, supporting information).

To get further insight, the visual evidences regarding the morphological transitions, are collected using optical microscopic studies. The typical micrographs for representative 0.25M TBAMES surfactant solution are shown in Figure 10. As evidenced from the micrographs at room temperature (Figure 10a), aggregates are very small and sizes are below the lower detection limit of the polarising microscope. However, near CP at 64°C, sizes are big enough and can now be seen by the polarizing optical microscopy (Figure 10b). Similar observations could be made for other surfactant solutions too. To get clear insight, the two phases at CP in 0.1M TBADS solution were separated and then analysed at RT. It was found that even at RT the rich phase showed the presence of bigger aggregates (Figure S12, supporting information) seen by POM unlike that with the lean phase which again on heating gave still the bigger aggregates in the visible range seen by the microscope. The grown micelles are clearly seen to be fusing with other micelles forming the bigger aggregates which are responsible for clouding phenomenon (Figure S13, supporting information). This is in agreement with the Langer-Schwartz theory⁵¹ that predicts: the nucleated phase may appear as a cloud of small droplets that grow slowly beyond the critical droplet size or it may form as an isolated droplet that rapidly grows to a very large size. Same analogy is drawn to the present surfactant solutions in which liquid-liquid immiscibility occurs above lower critical solution temperature (LCST) or CP.

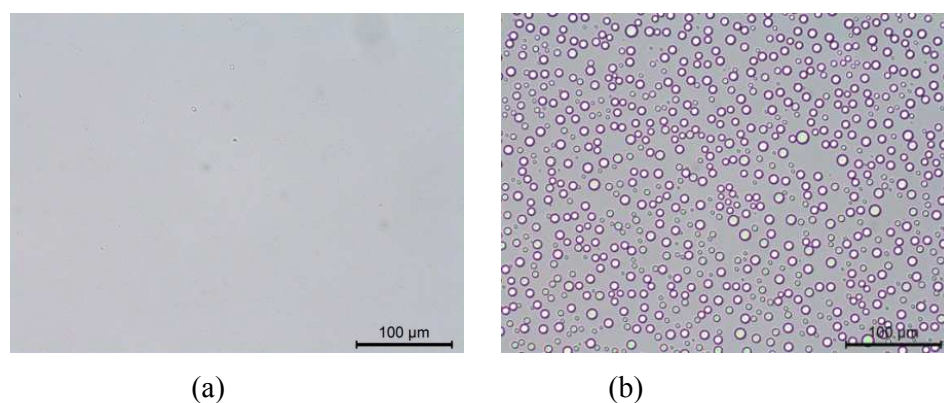


Fig. 10 Optical micrographs for 0.25M TBAMES at a) RT and b) near CP

Conclusion

This study focuses on several surprising and unexplained features of the temperature dependent self-assembly of anionic surfactants in aqueous solution. The solution behaviour of typical anionic surfactants, the involved morphological transitions (below and above CP) and the mechanism of clouding are explored by rationalizing the observations through experimental evidences along with the qualitative arguments using various physicochemical techniques. It is also found that nature of counterion and the head group part has a predominant role in deciding the micellar parameters, solution properties and the CP values. Attempt has been made to correlate the structure of ionic surfactant and the clouding phenomenon. Results of DLS, various NMR techniques, SANS and POM are in consonance with the micelle growth facilitated by dehydrated counterions and the surfactant head group. The fusion of these grown micelles result in bigger aggregates. Thus, the attractive interactions and the formation of bigger aggregates, as confirmed from NMR and POM results, respectively, are the two key factors involved in phase separation (clouding) of ionic surfactant solutions. The clouding in anionic surfactants in general and at low mole fractions (x) with TBP⁺ surfactants especially may find use as CPE systems for various charged species as well as thermally labile compounds such as vitamins and thermo-responsive drugs/proteins under ambient conditions.

ASSOCIATED CONTENT

Electronic Supplementary Information (ESI) available: Individual NMR spectra, NMR at variable temperature, 2D NOESY spectra, SANS spectra of different synthesized and some conventional surfactants (Figures S1-S13) and (Tables T1-T4) are available free of charge via the Internet at <http://pubs.rsc.org>.

AUTHOR INFORMATION

Corresponding author

E-mail: drksanjeev@gmail.com

Present address: Department of Applied Chemistry, The Maharaja Sayajirao University of Baroda, Vadodara 390 002, India.

ACKNOWLEDGMENT

The authors are thankful to UGC–DAE CSR, (CRS-151) Mumbai Centre, India and CSIR, New Delhi, India (Sanction No : 09/114/(0191)/2013-EMR-I) for the financial support. We also thank Dr. V. K. Aswal and Mr Sugam Kumar, Solid State Physics Division, BARC, Trombay, Mumbai, India for SANS analysis.

REFERENCES

1. D. Chandler, *Nature* 2005, **437**, 640–647.
2. S. Peleshanko, K. D. Anderson, M. Goodman, M. D. Determan, S. K. Mallapragada, V. T. Tsukruk, *Langmuir* 2007, **23**, 25–30.
3. D. J. Mitchell, G. J. T. Tiddy, L. Waring, T. Bostock, M. P. McDonald, 1983, **79**, 975-1000.
4. K. H. Gabor, C. Naomi, V. W. Ray, *Langmuir* 1996, **12**, 916-920.
5. S. R. Raghavan, H. Edlund, E. W. Kaler, *Langmuir* 2002, **18**, 1056-1064.
6. G. G. Waar, T. N. Zemb, M. Drifford, *J. Phys. Chem.*, 1990, **94**, 3086-3092.
7. S. A. Buckingham, C. J. Garvery, G. G. Waar, *J. Phys. Chem.*, 1993, **97**, 10236-10244.
8. B. L. Bales, R. Zana, *Langmuir* 2004, **20**, 1579-1581.
9. J. X. Xiao, G. X. Zhao, *Chin. J. Chem*, 1994, **12**, 552-554.
10. P. Mukherjee, S. K. Padhan, S. Dash, S. Patel, B. K. Mishra, *Adv. Colloid Interface Sci.* 2011, **162**, 59–79.
11. S. Kumar, A. Bhadoria, *J. Chem. Eng. Data* 2012, **57**, 521-525.
12. M. Benrraou, B. L. Bales, R. Zana, *J. Phys. Chem. B* 2003, **107**, 13432-13440.
13. B. L. Bales, M. Benrraou, K. Tiguida, R. Zana, *J. Phys. Chem. B* 2005, **109**, 7987-7997.
14. T. Ahmad, S. Kumar, Z. A. Khan, Kabir-ud-Din, *Colloids and Surfaces A: Physicochem. Eng. Aspects* 2007, **294**, 130-136.
15. J. H. Lin, W. S. Chen, S. S. Hou, *J. Phys. Chem. B* 2013, **117**, 12076-12085.
16. U. Thapa, J. Dey, S. Kumar, P. A. Hassan, V. K. Aswal, K. Ismail, *Soft Matter*, 2013, **9**, 11225-11232.
17. Y. Haiqing, Z. Zukang, H. Jianbin, Z. Rong, Z. Yongyi, *Angew.Chem. Int. Ed.* 2003, **42**, 2188-2191.

18. P. R. Majhi, A. Blume, *J. Phys. Chem. B* 2002, **106**, 10753-10763.
19. V. Yu, S. Bezzobotnov, L. Borbely, B. Cser, I. A. Farago, Y. Gladkih, M. Ostanevich, S. Vassi, *J. Phys. Chem.* 1988, **92**, 5138-5143.
20. S. Forster, T. Plantenberg, *Angew. Chem.*, 2002, **114**, 712-739.
21. J. Narayanan, E. Mendes, C. Manohar, *Int. J. Mod. Phys. B* 2002, **16**, 375-382.
22. S. J. Ryhanen, V. M. J. Saily, M. J. Parry, P. Luciani, G. Mancini, J. M. I. Alakoskela, P. K. J. Kinnunen, *J. Am. Chem. Soc.* 2006, **128**, 8659-8663.
23. S. D. Tanner, A. M. Ketner, S. R. Raghavan, *J. Am. Chem. Soc.*, 2006, **128**, 6669-6675.
24. S. Kumar, A. Bhadoria, H. Patel, V. K. Aswal, *J. Phys. Chem. B* 2012, **116**, 3699-3703.
25. R. Zana, M. Benrraou, B. L. Bales, *J. Phys. Chem. B* 2004, **108**, 18195-18203
26. V. K. Aswal, J. Kohlbrecher, *Chem. Phys. Lett.* 2006, **424**, 91-96.
27. Kabir-ud-Din, D. Sharma, Z. A. Khan, V. K. Aswal, S. Kumar, *J. Colloid Interface Sci.* 2006, **302**, 315-321.
28. A. Zilman, S. A. Safran, T. Sottmann, R. Strey, *Langmuir* 2004, **20**, 2199-2207.
29. T. J. Drye, M. E. Cates, *J. Chem. Phys.* 1992, **96**, 1367.
30. P. Panizza, G. Cristobal, J. Curely, *J. Phys.: Condens. Matter* 1998, **10**, 11659.
31. H. Bock, K. E. Gubbins, *Phys. Rev. Lett.* 2004, **92**, 135701-135704.
32. P. Yan, J. Huang, R. C. Lu, C. Jin, J. X. Xiao, Y. M. Chen, *J. Phys. Chem. B* 2005, **109**, 5237-5242.
33. G. C. Kalur, S. R. Raghavan, *J. Phys. Chem. B* 2005, **109**, 8599-8604.
34. Y. Yan, L. Li, H. Hoffmann, *J. Phys. Chem. B* 2006, **110**, 1949-1954.
35. Y. Sato, M. N. Shin-ichiro, K. Yoshikawa, *Chem. Phys. Lett.* 2003, **380**, 279-285.
36. V. K. Aswal, P. S. Goyal, *Curr. Sci.* 2000, **79**, 947-953.
37. J. B. Hayter, J. Penfold, *J. Colloid Polym. Sci.* 1983, **261**, 1022-1030.
38. S. H. Chen, T. L. Lin, In *Methods of Experimental Physics*, Price, D. L.; Skold, K. (Eds.) *Academic Press, New York*, 1987; Vol. 23, p 489.
39. S. Kumar, N. Parveen, Kabir-ud-Din, *J. Phys. Chem. B* 2004, **108**, 9588-9592.
40. S. Kumar, K. Parikh, *J. Surfact Deterg* 2013, **16**, 739-749.
41. L. J. Chen, S. Y. Lin, C. C. Huang, *J. Phys. Chem. B* 1998, **102**, 4350-4356.
42. C. V. Giongo, B. L. Bales, *J. Phys. Chem. B* 2003, **107**, 5398-5403.
43. B. W. Barry, R. Wilson, *Colloid Polym. Sci.* 1978, **256**, 251.
44. D. K. Rout, S. Chauhan, A. Agarwal, *Ind. Eng. Chem. Res.* 2009, **48**, 8842-8847.

45. J. N. Israelachvili, D. J. Mitchell, B. W. Ninham, *J Chem Soc, Faraday Trans 2* 1976, **72**, 1525-1568.
46. M. Villeneuve, R. Ootsu, M. Ishiwata, H. Nakahara, *J. Phys. Chem. B.* 2006, **110**, 17830-17839.
47. G. Karlstrom, *J. Phys. Chem.* 1985, **89**, 4962-4964.
48. S. Kumar, V. K. Aswal, A. Z. Naqvi, P. S. Goyal, Kabir-ud-Din, *Langmuir* 2001, **17**, 2549-2551.
49. R. J. Robson, E. A. Dennis, *J. Phys. Chem.* 1977, **81**, 1075-1078.
50. A. B. Mandai, S. Ray, A. M. Biswas, S. P. Mouiik, *J. Phys. Chem.* 1980, **84**, 856-859.
51. S. Langer, A. J. Schwartz, *Phys. Rev. A* 1980, **21**, 948-958.